

Low-temperature microwave response of barely metallic arsenic-doped silicon

K. J. Song* and T. G. Castner

Department of Physics and Applied Physics, University of Massachusetts Lowell, Lowell, Massachusetts 01854, USA

(Received 25 October 2004; published 2 August 2005)

Microwave measurements (frequency shifts and Q changes) of Si:As samples in the vicinity of the metal-insulator transition have been made with two different helical resonators and a cylindrical cavity in the frequency range 124 MHz to 13.9 GHz at temperatures to 1.5 K on samples from $0.72N_c$ to $2.45N_c$ [$N_c = 8.6 \times 10^{18}/\text{cc}$]. The resonators were calibrated with a constantan [$\text{Cu}_{0.55}\text{Ni}_{0.45}$] sample exhibiting close to Drude behavior. The measurements are in the regime $\hbar\omega < kT < (E_F - E_c) < \hbar\omega_p$ and are far into the Hagen-Rubens regime ($\omega\tau \ll 1$), but where the skin depth δ is less than the sample thickness t for metallic samples. Any significant “perfect conductor” contribution to $\Delta\omega/\omega$ is ruled out by calculations and the experimental results. The ratio $R = (\Delta\omega/\omega)/\Delta(1/Q)$ directly yields the transverse dielectric response $\varepsilon_t(N, \omega, T)$. The $\varepsilon_t(T \sim 1.5 \text{ K})$ values are consistent with a large Drude contribution $-(\omega_p\tau)^2$ plus a positive interband contribution primarily from $1s\text{-}A_1\text{-}1s\text{-}T_2$ impurity band transitions. The Drude component is consistent with the scaling behavior of $\sigma_{\text{dc}}(N, T \rightarrow 0)$.

DOI: 10.1103/PhysRevB.72.085204

PACS number(s): 71.30.+h, 71.45.Gm, 72.30.+q, 72.80.Cw

I. INTRODUCTION

One of the classical systems for the study of the metal-insulator transition (MIT) has been doped Si and Ge and numerous experiments have demonstrated the scaling behavior of the dc conductivity, the Hall coefficient, the conduction electron-spin resonance (CESR) excess linewidth, and the diffusivity $D(N_i, T \rightarrow 0)$ for metallic samples ($N > N_c$ where N_c is the critical density at $T=0$). These results have been discussed in various reviews.¹⁻³ For insulating samples ($N < N_c$) the characteristic temperatures T_0 and T_0' associated with Mott and Efros-Shklovskii variable range hopping (VRH) have been shown to scale to zero as $n \rightarrow n_c$. The critical behavior of VRH for these MIT systems has been discussed⁴ earlier. The dielectric response $\varepsilon(N, \omega, T)$ and microwave conductivity of barely metallic samples in the critical regime has not received attention although there have been several studies⁵⁻⁷ of the microwave behavior of insulating samples. Of particular relevance for this work are the infrared results⁸ of Gaymann *et al.* for Si:P which show both the expected plasma contribution consistent with Boltzmann-Drude (BD) behavior and the effect of interband transitions. Microwave measurements of amorphous $\text{Si}_{1-x}\text{Nb}_x$ very close to the critical point x_c have demonstrated⁹ $\sigma(\omega, T) \propto \omega^{1/2}$ in the quantum limit $\hbar\omega \gg kT$. There were early measurements¹⁰ of n and p -doped Ge that included metallic samples. Mahaffey and Jerde¹¹ reported results for N-ammonia solutions through the critical mole fraction showing large negative values of ε [$-10^2 < \varepsilon < -10^4$] characteristic of Drude behavior. This study presents results for Si:As showing the scaling behavior of the transverse dielectric response $\varepsilon_t(N > N_c, \omega, T)$ versus reduced density $N/N_c - 1$ in a frequency range where the response should contain a plasmon contribution plus an interband contribution. These results are consistent with $\varepsilon_t(N, \omega, T \rightarrow 0) \propto (N/N_c - 1)^p$ with $p = 0.3 \pm 0.1$ for $N/N_c - 1 < 1.0$, or in qualitative agreement with the scaling of $\sigma_{\text{dc}}(N, T \rightarrow 0)$. With the BD model this suggests the carrier relaxation time τ and the drift mobility in

zero magnetic field do not scale and that N_i , ω_p^2 , and σ_{dc} all scale with the same exponent.

Numerous microwave measurements have been made on semiconductors, ferrites, the high temperature superconductors as well as conventional superconductors, charge density wave systems, one-dimensional organic polymer systems, and two-dimensional electron (hole) systems by a variety of techniques and many of these measurements have been reviewed by Dressel and Grüner¹² (DG). The microwave measurements of superconductors requires high sensitivity to measure the small changes in absorption and changes in the complex surface impedance $Z_s = R_s + iX_s$ with temperature and Sridhar and Kennedy¹³ employed a high- Q superconducting cavity at 4.2 K [$Q_c > 10^7$] to measure $\text{Y}_1\text{Ba}_2\text{Cu}_3\text{O}_y$ and $\text{La}_{1.85}\text{Sr}_{0.15}\text{CuO}_4$ over a T -range 4.2 to 100 K employing a sapphire rod and a heater to vary the sample temperature. For barely metallic n -type Si samples the $\Delta(1/Q)$ and $\Delta\omega/\omega$ shifts are three orders of magnitude larger and adequate sensitivity is obtained from Cu wall resonators with Q 's at low- T of order 10^4 . We have employed both helical resonators (HR) [without the capacitive gap employed in the study of insulating Si:As and Si:P (Ref. 7)] and cylindrical cavity TE_{01n} modes. By placing the disk sample directly inside the helix centered on a lossless dielectric rod one can translate the sample between the nodes and antinodes of the field components inside the helical resonator (HR). With the disk samples of diameter d ($d/t > 40$) the E_r field plays the dominant role in determining $\Delta\omega/\omega$ in the HR while for the cylindrical cavity (CC) TE_{01n} modes E_θ is the dominant field component.

The characteristic energies for barely metallic samples are the Fermi energy $\varepsilon_F = E_F - E_c$ (E_c the mobility edge), the thermal energy kT , the plasma energy $\hbar\omega_p$, and the photon energy. The data described herein are in the regime $\hbar\omega < kT < \varepsilon_F < \hbar\omega_p$. Since both ε_F and ω_p scale to zero as $N \rightarrow N_c$ one cannot approach N_c too closely to keep $kT \ll \varepsilon_F$ (for $T_{\text{min}} = 1.5 \text{ K}$ and $N_{\text{min}} = 1.05N_c$ $kT_{\text{min}}/\varepsilon_{F\text{min}} \sim 0.1$ for Si:As). For $\hbar\omega \ll kT$ the diffusive correction from e - e interactions

is negligible.¹⁴ The data measured cover a range 124–2010 MHz in two different helical resonators (HR) and to 13.9 GHz with a CC. At 13.9 GHz and 1.5 K $\hbar\omega/kT \sim 0.4$. For all metallic samples, ω , and T , $\omega\tau \ll 1$ [Hagen-Rubens regime], suggesting no ω -dependence from the Drude model itself. However, there can be $\delta\sigma(N, \omega, T)$ corrections from e - e interactions, interband transitions, or from insulating portions of the sample within a skin depth δ or so of the surface. Frequency measurements probe a length scale $L_\omega = (D/\omega)^{1/2} = \ell/(3\omega\tau)^{1/2}$ where D is the diffusivity ($D = v_F^2\tau/d$ for a degenerate metal and the mean-free-path $\ell = v_F\tau$). All the measurements are in the classical regime $\ell \ll L_\omega \ll \delta = (2/\mu\sigma\omega)^{1/2}$. The metallic sample data is in the skin depth regime $\delta < t$, where t is the disk sample thickness. As N decreases toward N_{\min} δ approaches t and corrections are required resulting from interference between the waves entering the two flat surfaces of the disk. These corrections have been calculated¹⁵ and are negligible for $\delta < t/5$ (i.e., the 13.9 GHz CC data).

II. BACKGROUND

Microwave measurements in the low frequency Hagen-Rubens regime ($\omega\tau \ll 1$) for metals would normally be in the classical skin depth regime. In this regime the complex conductivity $\sigma = \sigma_1 + i\sigma_2$ and dielectric response $\varepsilon = \varepsilon_1 + i\varepsilon_2$ [$\varepsilon_1 = 1 - 4\pi\sigma_2/\omega$; $\varepsilon_2 = 4\pi\sigma_1/\omega$] of metals is to be given approximately by Boltzmann-Drude behavior with possible corrections to ε_1 from interband contributions. DG refer to this classical regime as the homogeneous limit where the dependence of $\sigma(\mathbf{q}, \omega)$ on \mathbf{q} is very small and give the expression

$$\sigma(\mathbf{q}, \omega) = (N_i e^2 \tau / m^*) [1 / (1 - i\omega\tau)] \times [1 - 1/5(qv_F\tau)^2 / (1 - i\omega\tau)^2 + \dots], \quad (1)$$

where the correction to Drude behavior depending on $qv_F\tau \approx \ell/\delta$. For the Si:As metallic samples studied in this work $0.002 < \delta < 0.02$ cm and $0.8 < \ell < 4$ nm and $qv_F\tau < 2 \times 10^{-4}$. Hence standard \mathbf{q} -dependent corrections to Drude theory are totally negligible, however, other corrections might arise because of the fact the samples are inhomogeneous just above the critical density n_c and because of interband corrections to $\varepsilon_1(N, \omega, T)$ from low-lying excited states. In general one expects to have

$$\varepsilon_1 = \varepsilon_h - (\omega_p\tau)^2 / [1 + (\omega\tau)^2] + \delta\varepsilon_{\text{ib}}(N, \omega, T), \quad (2)$$

where ε_h is the host dielectric constant and the interband contribution $\delta\varepsilon_{\text{ib}}$ can only be ascertained from a Kramers-Kronig analysis of the interband conductivity $\delta\sigma_{\text{ib}}(N, \omega', T)$.

In the Hagen-Rubens regime the plasmon Drude contribution $-(\omega_p\tau)^2$ to ε_1 depends critically on the collision time, which might be different from the bulk τ which enters $\sigma_{\text{dc}} = N_i e^2 \tau / m^*$ because of extra surface scattering. Table I shows the relevant parameters for Cu, Al, constantan, Si:As, and Si:P where $r_s = (3/4\pi N_i)^{1/3}$, $a_0 = \hbar^2 / me^2$, $\omega_p^2 = 4\pi N_i e^2 / m^*$, and $\rho_{\mu\Omega}$ is the bulk resistivity in micro ohm cm [as $T \rightarrow 0$ for Si:As and Si:P]. N_i is the density of itinerant electrons. The values of $\omega_p\tau$ for Cu and Al are overestimates because of the use of the bulk τ from σ_{dc} . The Cu and Al values are in-

TABLE I. Plasmon parameters for various metals.

	r_s/a_0	$\rho_{\mu\Omega}$	m^*/m	$\omega_p\tau$	$(\omega_p\tau)^2$
Cu (RT)	2.67	1.6	1.3	490	2.4×10^5
Al (RT)	2.07	2.5	1.4	222	4.9×10^4
Cu _{0.55} Ni _{0.45}	4.13	52	1.3	29	842
SiAs ($2N_c$)	45.4	2777	0.26	8.86	78.6
SiP ($2N_c$)	60.0	3846	0.26	9.70	94.1

cluded since they were measured by Diehl, Wheatley, and Castner¹⁶ (DWC) and Song and Castner (SC).¹⁵ However, Cu_{0.55}Ni_{0.45} samples were used for the calibration because they led to more accurate measurements of $\Delta(1/Q)$ than the Cu and Al samples and ought to closely exhibit Drude behavior. For Cu_{0.55}Ni_{0.45} $\rho_{\mu\Omega}$ is very weakly dependent on T (always in the classical skin depth regime at all T) and $(\omega_p\tau)^2$ is only about one order of magnitude larger than for SiAs and SiP.

A. The expression for the frequency shift produced by a sample

Using Maxwell's equations with and without a sample Müller¹⁷ derived an early expression for the frequency shift when a sample is placed inside a resonant cavity. This expression also arose independently during World War II (MIT Rad. Lab¹⁸ and Cornell¹⁹ reports). The derivation has been given by Hauser,²⁰ who termed the expression the ‘‘Beth-Schwinger’’ expression. The fractional frequency shift produced by a sample is

$$\frac{\omega - \omega_0}{\omega} = - \frac{\int_s [\mathbf{E}_0 \cdot \Delta\boldsymbol{\varepsilon} \cdot \mathbf{E} + \mathbf{H}_0 \cdot \Delta\boldsymbol{\mu} \cdot \mathbf{H}] dV}{\int [\varepsilon_0 \mathbf{E}_0 \cdot \mathbf{E} + \mu_0 \mathbf{H}_0 \cdot \mathbf{H}] dv}, \quad (3)$$

where \mathbf{E}_0 and \mathbf{H}_0 are the fields without the sample (ω_0) and \mathbf{E} and \mathbf{H} are the fields after the sample is added (ω). $\Delta\boldsymbol{\varepsilon} = (\boldsymbol{\varepsilon} - 1)\boldsymbol{\varepsilon}_0$ while $\Delta\boldsymbol{\mu} = (\boldsymbol{\mu} - 1)\boldsymbol{\mu}_0$ are only nonzero inside the sample and the \int_s in the numerator is only over the sample. The denominator in Eq. (3) is just the stored energy W inside the HR. For paramagnetic metals and doped semiconductors the magnetic susceptibility will be very small and the magnetic contribution to $(\omega - \omega_0)/\omega$ will be negligible because $\Delta\boldsymbol{\mu} = 4\pi\chi\boldsymbol{\mu}_0$ is so small. In two early semiconductor studies^{21,22} only $\Delta(1/Q)$ was measured for spherical samples in order to determine the resistivity at room temperature in the skin depth regime at X-band frequencies. No effort was made to determine the frequency shift in these studies. The magnetic term in \int_s in W_s is negligible. The paramagnetic metal case [$\chi < 10^{-6}$] differs substantially from the ferrite case^{23–26} [NiZn, MnMg, etc.] studied extensively after World War II. For the ferrite case $\Delta\boldsymbol{\mu}$ was large and samples (both spheres and disks) were placed at an \mathbf{H} antinode. The objective was to determine the tensor components of χ (rather than ε). Spencer *et al.*²⁷ and also Waldron²⁸ have considered the criteria for the applicability of cavity perturbation theory

represented by Eq. (3). Spencer *et al.* concluded that the earlier criterion on the stored energy $\Delta W/W \ll 1$ was too strong and that a weaker criterion $\Delta\omega/\omega \ll 1$ is sufficient. Waldron mentions the sample shape dependence and that spherical samples must be kept away from the cavity walls to avoid reflection effects on \mathbf{E} and \mathbf{H} . For disk samples he suggests \mathbf{E} and \mathbf{H} cannot be accurately determined, except in the limit of zero thickness. He notes the approximation that \mathbf{E} in the disk is the same as \mathbf{E}_0 in the absence of the disk. However, at the surface of the disk SC¹⁵ employed for the tangential component $\mathbf{E}_t(r,z) = \mathbf{E}_{0,t}(r,z)$ and for the normal component $\mathbf{E}_n(r,z) = \mathbf{E}_{0,n}/\epsilon_n$ from the conventional boundary conditions on \mathbf{E} (also \mathbf{H}). This is nearly the same as Waldron's discussion for $\epsilon_n \gg 1$. Waldron notes the disk thickness/diameter ratio t/d needs to be kept small. In our case $t/d < 0.01$ for the Cu_{0.55}Ni_{0.45} calibration sample and $t/d < 0.03$ for the metallic Si:As samples. The fields \mathbf{E} and \mathbf{H} decay rapidly for the skin depth $\delta < t$ and lead [see SC¹⁵ and Eq. (13a) below] to $\Delta\omega/\omega \propto -(\epsilon_t - 1)\delta$ for $\delta \ll t$ rather than the $\Delta\omega/\omega \propto V_s/V_c = (d/a)^2 t/L$ dependence.

Even though the fields can change outside the sample because of currents and charges inside the sample these changes in \mathbf{E} and \mathbf{H} outside the sample make no contribution to the numerator in Eq. (3). Since $(\epsilon - 1)$ can be very large and negative for a good metal (-3.37×10^4 for Al at 293 K) from the plasma contribution this leads to large positive frequency shifts that are much larger than the filling factor V_s/V_{HR} . It is this argument and the associated experimental results for metals that conflict with the "perfect conductor" contribution $(\omega - \omega_0)/\omega_0]_{pc}$ discussed by many authors.²⁹⁻³³ From Eq. (3) it might appear that there is no contribution to the frequency shift from the interior of the metal where \mathbf{E} and \mathbf{H} are 0, namely when the sample thickness $t \gg \delta$. Significant attention has to be given to the "perfect conductor" contribution²⁹⁻³³ to the frequency shift. Klein *et al.*³¹ give the expression

$$\Delta\omega/\omega_0 = \xi Z_s + \lim_{|\sigma| \rightarrow \infty} \Delta\omega/\omega_0, \quad (4)$$

where ξ is the resonator constant and the second term represents an additive constant representing the excluded volume of the field by the sample as the sample approaches the perfect conductor limit. This term is known for a sphere and is given by $1.5A(V_s/V_c)$ where A is a constant of order unity depending on the field configuration. This result predicts a result proportional to the volume V_s of the sample. However, this prediction is at odds with data for Cu disks (DWC).¹⁶ Furthermore, Eq. (3) produces a result much larger than the second term in Eq. (4) that is proportional to $|\epsilon_1 - 1|\delta$. Within the Drude model this term continues to increase as $\sigma \rightarrow \infty$ even as $\delta \propto (\sigma)^{-1/2} \rightarrow 0$. However, within the Drude model there is a minimum δ_{\min} of order of the plasma wavelength. The various problems with the "perfect conductor" approximation will be discussed elsewhere in more detail.

The resonant frequencies ω_0 given in E&M texts for a cavity resonator are given for the perfect conductor case ($\delta = 0$). For normal conductor (Cu) walls with a finite δ one can calculate the downward frequency shift $\omega_a - \omega_0$

$= -(1/2\sigma\delta)[\int_s H_t^2 ds / \int \epsilon_0 E^2 dV]$. For the cylindrical cavity TE_{01n} modes this yields

$$(\omega_a - \omega_0)/\omega_0 = -(1+i)(\delta/2)[(k_1/k)^2/a + (k_3/k)^2/L], \quad (5)$$

where a is the radius and L the length and $k_1 = 3.832/a$ and $k_3 = n\pi/L$ with $k^2 = k_1^2 + k_3^2$. For the TE₀₁₂ mode with $\delta_{Cu(RT)}/2a = 1.5 \times 10^{-5}$ the fractional frequency shift is less than 1.2×10^{-5} . The imaginary part of Eq. (4) $[\omega - i\alpha]$ leads to the Q_0 of the resonator such that $1/Q_0 = \text{Im}(\omega_a - \omega_0)/\omega_0$. This frequency shift is negligible compared to the measured fractional shifts of order 10^{-2} . Note that the empty cavity frequency is this ω_a . Such shifts also occur for the HR, but are much harder to calculate. They are negligible compared to the measured frequency shifts and those calculated from Eq. (3).

B. The perfect conductor scenario ($\delta = 0$)

Slater²⁹ has given the expression $\omega^2 = \omega_a^2 [1 + \int (H_a^2 - E_a^2) dV]$ where the integral is over the perturbed boundary. If the perturbed boundary is a region where H_a is large and E_a near zero one will get a positive frequency shift. In the opposite limit $H_a \sim 0$ and E_a is large one gets a negative shift. In this approach it is the excluded field that determined the frequency shift. If one employs the Slater expression one obtains a shift $(\omega - \omega_a)/\omega_a = A(V_s/V_c)$ when H_a is a maximum, V_s/V_c is the filling factor of the sample with volume V_s in a resonator of volume V_c . A is a coefficient of order unity which depends on the integration over H_a^2 . For the fields in a cylindrical cavity for TE_{01n} modes one calculates this "perfect conductor" diamagnetic contribution $[\mu = \mu_0(1 + \chi_m) = 0, \chi_m = -1]$ using Eq. (3) and the field $H_z = (k_1/k)J_0(k_1 r) \sin k_3 z$ ($k_1 = 3.832/a$, $k_3 = n\pi/L$ for a cylinder or radius a and length L). At the antinode [$k_3 z = (\pi/2)$, etc.] one obtains the result for a disk sample of radius r_s and thickness t

$$\Delta\omega/\omega_{pc}] = (r_s^2/a^2)(t/L)\{[J_0^2(k_1 r_s) + J_1^2(k_1 r_s)]/J_0^2(k_1 a)\}(k_1/k)^2, \quad (6)$$

where $k_1^2 + k_3^2 = k^2$. For our Cu_{0.55}Ni_{0.45} with $k_1 r_s = 1.12$ the coefficient of V_s/V_c is 4.5. This is to be compared with a diamagnetic shift $2.47 V_s/V_c$ obtained by Zhai *et al.*³³ for a spherical sample placed at the center of the TE₀₁₁ mode. For $V_s/V_c = 2.5 \times 10^{-4}$ one obtains fractional frequency shifts of 9.4×10^{-4} , 6.5×10^{-4} , and 4.4×10^{-4} for the modes $n=1$, $n=2$, and $n=3$, respectively. These shifts are not totally negligible but are less than 2% of the observed frequency shifts. Note that if one used the susceptibility $\chi_m < 10^{-6}$ characteristic of a real paramagnetic metal any magnetic field contribution from Eq. (3) would be totally negligible compared to electric field contributions. In addition for real metals with a skin depth δ the field would only be excluded in an effective thickness $t_{\text{eff}} = t - 2\delta$.

Equation (3) can be employed to obtain the diamagnetic $(\omega - \omega_0)/\omega$ contribution for a cylindrical cavity with the perfect diamagnet of radius a^- placed at $z=0$ where the only TE_{01n} mode field is H_r . The result is $\Delta\omega/\omega = (k_3/k)^2(t/L)$, which is the identical result obtained from the frequency ex-

pression for the TE_{01n} modes when the length is shortened from L to $L-t$ for $t \ll L$. On the other hand if the same sample is placed at the antinode of E_θ (H_z) the diamagnetic contribution is $(k_1/k)^2(t/L)$. For a real metal with finite σ and skin depth δ the E_θ contribution is $|\varepsilon_t - 1|(2\delta/L)$ and the diamagnetic contribution is reduced from t to $t - n\delta$ where $n \approx 2$. The ratio for a real metal is the $|\varepsilon_t - 1|(\delta/t)/(k_1/k)^2$, which will be much larger than 1 when $|\varepsilon_t - 1|(\delta/t) \gg 1$. For the samples employed in this research with $r_s/a = 0.293$ the “perfect conductor” diamagnetic contribution is $4.5(r_s/a)^2(t/L)(k_1/k)^2$. The $\Delta\omega/\omega$ from the first term in Eq. (3) would indeed be less than the diamagnetic contribution if one used a “spherical” sample with $d \approx t$. However, with the disks employed with $d/t \sim 110$ for $Cu_{0.55}Ni_{0.45}$ and 35–45 for the SiAs samples the diamagnetic contribution to $\Delta\omega/\omega$ is small, but not totally negligible. The data presented in DWC for Cu disks (see Fig. 11) of thickness t in a HR showed $\Delta\omega/\omega \propto d^p$ for $4.76 < d < 11.1$ mm with p increasing from 3.5 to 3.8. DWC concluded this result was consistent with the field E_r in the HR plus a rim correction (d^3t). DWC in Fig. 10 also showed small thickness corrections for HR modes $n=1$ and $n=2$ for Cu disks of constant d and t ranging from 0.126 to 0.508 mm. If the “perfect conductor” diamagnetic contribution was dominant one would have had $[\Delta\omega/\omega]_{pc} \propto t$. The DWC data forces one to conclude the diamagnetic contribution is small.

The fields for a perfect infinite helix have been given by Pierce³⁴ and are readily adapted for the standing wave case. There are no pure transverse TE or TM modes. The great advantage of the HR is the nondegenerate modes. However, the fields inside the HR are complicated by the finite length, the conducting end plates, and the fact that one end of the helix is shorted to the Cu shield. It is these complications that require the use of appropriate metals to calibrate the HR.

Ong³⁵ has calculated $\Delta\omega/\omega$ for an isotropic ellipsoidal shaped sample in a CC in the skin depth regime starting with the “Bethe-Schwinger” expression. Ong employs the depolarization factor N analogous to the extended quasistatic (EQS) case of Champlin and Krongard³⁶ and obtains the result

$$\alpha/N_z + \Delta\omega/\omega = -\Delta(1/2Q), \quad (7)$$

where $\alpha = \varepsilon_0 E_0^2 V_s / 4W$ and N_z is the depolarization factor in the \mathbf{z} direction ($\mathbf{E}_0 \parallel \mathbf{z}$, but in our case \mathbf{E}_0 is transverse and \parallel to \mathbf{r} or $\boldsymbol{\theta}$). In the good metal limit $\Delta(1/2Q) \ll \Delta\omega/\omega$ and Ong’s result leads to $\Delta\omega/\omega \approx -\alpha/N_z$, which is very different from the result we obtain starting with Eq. (3). For Ong’s TTF-TCNQ case $\alpha/N_z \approx 1.8 \times 10^{-4}$, or a factor of 100 smaller than our Si:As values. However, our result for $\Delta(1/Q)$ is consistent with Ong’s result [his Eq. (36)]. Our treatment (SC¹⁵) matches boundary conditions ($\mathbf{E}_{0,t} = \mathbf{E}_r$, corresponding to $N_t = 0$; $\mathbf{E}_{0,z} = \varepsilon_t \mathbf{E}_z$ and $N_z \approx 1$) and predicts the very large $\Delta\omega/\omega$ that are observed. For our case ε is a tensor and our results appear inconsistent with Eq. (11) in Ref. 35.

C. The $1/Q_s$ loss due to the sample

The most common approach to the calculation of $1/Q_s$ is to determine the imaginary part of $\Delta\omega/\omega$, as calculated from

Eq. (3). In many cases this may be a reasonable approximation, but it may not be correct when the fields \mathbf{E} and \mathbf{H} differ substantially from \mathbf{E}_0 and \mathbf{H}_0 in Eq. (3). When one inserts a metal sample into a resonant cavity there can be substantial changes in the fields which may be hard to accurately determine. In general one expects

$$1/Q_s = TP_{\text{dis}}/W = (2\pi/\omega W)R_s \int H_t^2 ds, \quad (8)$$

where T is the period, P_{dis} is the power dissipated, R_s is the surface impedance ($1/\sigma\delta$ in the classical skin depth regime), and H_t is the transverse magnetic field at the surface of the metal sample. The stored energy is now $\mathbf{W} \approx \varepsilon_0 \int \mathbf{E}^2 dv + \mu_0 \int \mathbf{H}^2 dv + (\varepsilon - \varepsilon_0) \int_s \mathbf{E}^2 dV + (\mu - \mu_0) \int_s \mathbf{H}^2 dV$, where the latter two integrals are usually negligible when the skin depth δ is negligible compared to other dimensions. This stored energy differs from the denominator in Eq. (3) and the difference grows as \mathbf{E} and \mathbf{H} differ from \mathbf{E}_0 and \mathbf{H}_0 . When a metallic sample is at the antinode of E_θ and H_z for TE_{01n} modes in a cylindrical cavity one has H_t in Eq. (5) given by $H_t = 1/R_s E_t$ (H_r and E_θ) which is required to have a Poynting vector into the metallic disk. In the absence of the metallic sample at this antinode H_r would be zero and $E_\theta = E_{\theta,0}$. It is more difficult to determine exactly how E_θ changes in the presence of the metallic disk sample but if E_θ still behaves as the fields do in a cylindrical cavity there will be no change in the fractional frequency shift given by Eq. (3) because both numerator and denominator will be changed by the same amount. At this antinode the drastic change in the field is the H_r necessary for a nonzero P_{dis} . On the other hand, if the metallic disk is positioned at the node of E_θ and H_z (antinode of H_r) then the drastic change in the fields will be in E_θ .

With a metallic disk in a cylindrical cavity at the antinode of E_θ (H_z) a circular current is induced in the metallic disk which leads to a magnetic dipole \mathbf{m} normal to the disk. The fields from this oscillating dipole are determined from the vector potential $A_\theta = (\mu_0 m / 4\pi) r / (r^2 + z^2)^{3/2}$ and $\mathbf{B} = \text{curl } \mathbf{A}$ and $E_\theta = -\partial A_\theta / \partial t$. These fields make no contribution to the numerator in Eq. (3), nor to the dissipation P_{dis} in Eq. (7) because E_θ from \mathbf{m} is out of phase with the original $E_{\theta,0}$ in the cylindrical cavity and B_r from \mathbf{m} is zero in the plane of the sample ($z=0$). However, these fields are not small and can contribute to the stored energy W in Eq. (8) but will not contribute to the denominator in Eq. (3). For a good conductor at microwave frequencies the fields from the dipole can be big enough at microwave frequencies to constitute an important correction to the calculation of $1/Q_s$. This induced dipole field is drastically reduced in the HR because the principal transverse E -field is E_r , which yields radial currents and no dipole \mathbf{m} . The very much smaller E_θ is of magnitude $(v_p/c)E_r$ and is reduced by the factor $v_p/c = 0.018$ for the larger HR. This is one of two significant advantages of the HR, namely (1) the principal \mathbf{E} field component is E_r , which does not lead to an induced magnetic dipole in a metallic disk, and (2) that the HR modes are nondegenerate and well separated, in contrast to the TE_{01n} and TM_{11n} of a cylindrical cavity. In addition the HR, as a slow wave device, allows microwave measurements to be made at low-temperature

with reasonable length scales down to the hundreds of MHz regime. The offsetting complication is the more complex fields within the HR and the need to calibrate it with some well characterized metal.

D. Impedance approach to resonant circuit analysis

DG have given a description in terms of the impedance of the sample $Z_s = R_s + iX_s$ placed in a resonant circuit with a characteristic impedance $Z_c = (L/C)^{1/2}$ and an unperturbed resonant frequency ω_0 . R_s is the surface resistance of the sample while X_s is the surface reactance. When the frequency changes from ω_0 to ω and the quality factor from Q_0 to Q it is possible to relate these changes to R_s and X_s giving

$$(\omega - \omega_0)/\omega_0 = X_s/Z_c g_0 \quad (9)$$

and

$$\Delta(1/Q) = 1/Q - 1/Q_0 = 2R_s/Z_c g_0.$$

Note that the ratio of $\Delta\omega/\omega_0$ to $\Delta(1/Q)$ yields $X_s/2R_s$, which is a characteristic of the sample and is independent of the resonant circuit characteristic impedance Z_c and the geometric factor g_0 which depends on the size and shape of the resonator and sample. Z_s can be expressed in terms of the complex conductivity of the sample $\sigma_1 + i\sigma_2$. Neglecting magnetic effects [$\mu \approx \mu_0$] one obtains $Z_s = [\mu_0\omega/ci(\sigma_1 + i\sigma_2)]^{1/2}$ and this result allows a determination of R_s and X_s . The ratio X_s/R_s is

$$\begin{aligned} -X_s/R_s &= \{[(\sigma_1^2 + \sigma_2^2)^{1/2} + \sigma_2]/[(\sigma_1^2 + \sigma_2^2)^{1/2} - \sigma_2]\}^{1/2} \\ &= [(1 + \sin 2\beta)/(1 - \sin 2\beta)]^{1/2}, \end{aligned} \quad (10)$$

where $\sin 2\beta = \sigma_2/(\sigma_1^2 + \sigma_2^2)^{1/2}$. The ratio for a good metal in the Hagen-Rubens regime ($\omega\tau \ll 1, \sigma_2 \ll \sigma_1$), the ratio $r(\omega\tau)$ in Eq. (10) approaches unity. However, the ratio $R = (\Delta\omega/\omega)/\Delta(1/Q)$ obtained with the Bethe-Schwinger expression in Eq. (3) yields $R \propto 4\pi\sigma_2/\omega = 1 - \epsilon_1$. This differs from the ratio in Eq. (10). The experimental values R_{expt} for various good metals and for the MIT system Si:As will be compared with these two different theoretical expressions. One can separately solve of X_s and R_s to obtain

$$X_s = -1/\delta(\sigma_1^2 + \sigma_2^2)^{1/2} \quad (11)$$

and

$$R_s = r(\omega\tau)/\delta(\sigma_1^2 + \sigma_2^2)^{1/2},$$

where the skin depth $\delta = c/\{2\pi\mu\omega[(\sigma_1^2 + \sigma_2^2)^{1/2} + \sigma_2]\}^{1/2}$. The difference between the fractional frequency shift in Eq. (9) and the Bethe-Schwinger result is that X_s in Eq. (11) is not proportional to σ_2 .

III. EXPERIMENTAL DETAILS

Many of the experimental details are given in SC and in DWC. However, a second smaller HR was constructed and used for measurements in the 440 to 2800 MHz regime (modes $n=1-4$). Furthermore, SC did not discuss the calibration of the Q -change $\Delta(1/Q)$ because the Q changes were

TABLE II. Si:As samples studied.

	t (mm)	d (cm)	ρ_{RT} (Ω cm)	N/N_c
C16	0.519	1.0790	0.0093	0.72
D7	0.381	1.1458	0.0075	1.051
D2'	0.295	1.1429	0.00735	1.062
E14	0.335	1.1480	0.0070	1.099
D14	0.330	1.1445	0.00695	1.108
F4	0.312	1.1443	0.0068	1.137
G7	0.348	1.1387	0.0066	1.174
B18	0.284	1.1455	0.0044	1.993
A2	0.254	1.1463	0.0033	2.486

very small for Cu, Al, and Au. It was found necessary to calibrate the HR [both $\Delta\omega/\omega$ and $\Delta(1/Q)$] with a much poorer conductor, but one that might be expected to show Drude behavior in the frequency range of the measurements. Constantan [$\text{Cu}_{0.55}\text{Ni}_{0.45}$] was chosen because of its larger resistivity ρ that is virtually independent of T , but which also remains in the classical skin depth regime over the entire T -range from RT to 1.5 K. Measurements were also made in a cylindrical cavity which was obtained by removing the helix from the HR and employing an insulated end plate to help damp out the TM_{1ln} modes. The D/L ratio was selected to minimize mode overlap. Measurements were made for other TE_{1ln} modes, but only the TE_{01n} mode results in the frequency range 11.2 to 16.8 GHz will be discussed. These data was obtained with a Hewlett-Packard 8750A network analyzer.

A. Samples

The disk samples were prepared with diamond coring bits and were selected from 5.08 cm diameter wafers used in previous dc transport studies.³⁷ Each wafer was profiled with ρ_{RT} measurements and an effort was made to select portions of the wafer with uniform ρ_{RT} values. Both the outer diameter and the inner hole (0.317 cm diam) were cut at the same time to improve concentricity of the two circles. This ruled out making 4-point probe ρ_{RT} measurements on the final sample. The samples were then etched with a standard CP-4 etch. The samples and their characteristics are listed in Table II. The samples in Table II were measured in the larger HR ($V_{\text{HR}} = 47.24 \text{ cm}^3$) and many of them also in the cylindrical cavity. A second set of smaller samples ($d = 0.61 \pm 0.01 \text{ cm}$, $0.289 < t < 0.350 \text{ mm}$) was prepared for measurement in the smaller HR ($V_{\text{HR}} = 5.147 \text{ cm}^3$). In most cases these samples were cut from the same wafer as those in Table II and had nearly the same values of ρ_{RT} .

IV. EXPERIMENTAL RESULTS

Figure 1 shows the results for $f(z) - f_0$ and $\Delta(1/Q)$ for the $\text{Cu}_{0.55}\text{Ni}_{0.45}$ calibration sample at 77 K for the large HR near the maximum f_{max} and the minimum f_{min} for HR modes 2, 3,

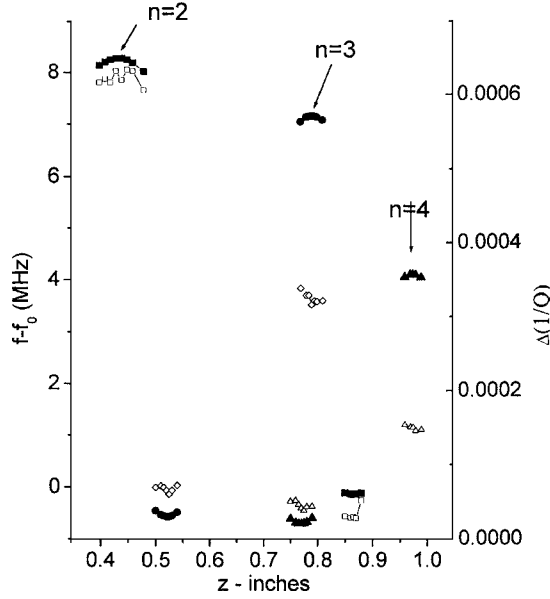


FIG. 1. $f(z)-f_0$ (closed symbols) and $1/Q(z)$ (open symbols) vs z for the larger HR modes $n=2-4$ for a $\text{Cu}_{0.55}\text{Ni}_{0.45}$ sample. The empty HR frequencies f_0 : $n=2$, 364.23 MHz; $n=3$, 596.25 MHz; and $n=4$, 797.13 MHz. The upper values are at E_r and the lower values are at $E_r=0$. Note that the values of $f-f_0$ at the E_r node are slightly negative consistent with Eq. (4b) in SC.

and 4. The scatter for the $\Delta(1/Q)$ values is much greater than for $f-f_0$. Within the experimental uncertainties the values of $\Delta(1/Q)_{\max}$ closely coincide with the value $f_{\max}-f_0$. Figure 2(a) gives $f-f_0$ and $1/Q(z)$ for the TE_{011} and TE_{012} modes for the cylindrical cavity [$D/L=1.02$]. The $f(z)-f_0$ values are very accurate while the $1/Q(z)$ values show a lot of scatter resulting from the partial overlap of the TE_{01n} and TM_{11n} modes (and possibly other modes) at certain values of z which can significantly lower the values of $Q(z)$. Note also that as the sample approaches a wall [$z=0$] or the coupling probes [$z=1.3$ in.] the $1/Q(z)$ values are dramatically increased. To obtain accurate values of $1/Q(z)$ for the TE_{01n} modes one must only take the smallest values $1/Q(z)$ and fit these values to the expression

$$1/Q(z) = 1/Q_s [(f(z) - f_{\min}) / (f_{\max} - f_{\min})] + 1/Q_0, \quad (12)$$

where Q_s is the sample Q , Q_0 is the empty cavity Q , and the $[\] \approx \cos^2(nz/L)$. Analysis of the data in Fig. 2(a) with Eq. (11) yields $Q_0(\text{TE}_{011})=17,700$ and $Q_0(\text{TE}_{012})=21,900$ at 77 K. The ratio of these two values is in good agreement with the calculated ratio for these two modes. An effort was made to obtain data for the TE_{013} mode but the mode overlap was more serious and the errors in $1/Q(z)$ were significantly larger. From values of Q_s and $(f_{\max}-f_0)/f_{\max}$ the ratio $R = (\Delta f/f) / \Delta(1/Q)$ as well as the calibration coefficients I and K' are obtained (see Table III). Figure 2(b) gives $f(z)-f_0$ and $\Delta(1/Q) = 1/Q(z) - 1/Q_0$ for the smaller HR for modes $n=3$ and $n=4$. For mode $n=3$ we chose the large peak at $z \sim 0.34$ in. for calibration, while for mode $n=4$ we chose the peak at $z \sim 0.43$ in. The calibration is most accurate for

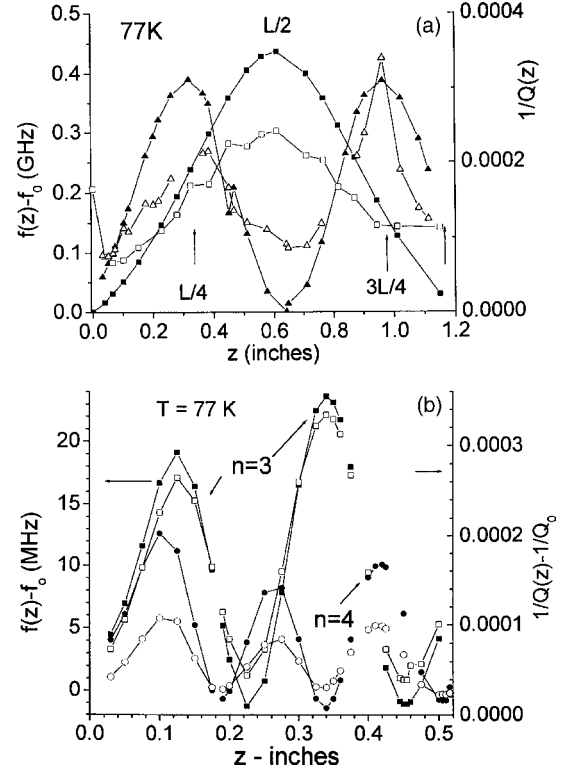


FIG. 2. $\text{Cu}_{0.55}\text{Ni}_{0.45}$ calibration samples: (a) $f(z)-f_0$ and $1/Q(z)$ vs z for the CC for modes TE_{011} and TE_{012} . The variations in $\Delta(1/Q)$ result from mode overlap with other modes. (b) $f(z)-f_0$ and $1/Q(z)-1/Q_0$ vs z for the smaller HR for modes $n=3$ ($f_0 = 1987.05$ MHz) and $n=4$ ($f_0 = 2810.27$ MHz).

modes 2 and 3 and less accurate for $n=4$ because $\Delta(1/Q)$ is smaller for the higher n modes.

The data has been analyzed with the expressions

$$\begin{aligned} \Delta\omega/\omega &= (f_{\text{an}} - f_0)/f_{\text{an}} \approx -(\epsilon_t - 1) \delta F_\epsilon(t/\delta) \int_s \mathbf{E} \cdot \mathbf{E}_0 dA_s / U \\ &= -(\epsilon_t - 1) \delta F_\epsilon(t/\delta) I, \end{aligned} \quad (13a)$$

TABLE III. Calibration coefficients from $\text{Cu}_{0.55}\text{Ni}_{0.45}$ samples.

Device	K' (cm^{-1}) ^a	R	I (cm^{-1}) ^b
Large HR $n=2$	$0.341 \pm .005$	34.9 ± 0.4	0.0141
$n=3$	$0.202 \pm .011$	40.2 ± 2	0.00954
$n=4$	$0.105 \pm .009$	41.9 ± 3	0.00522
Small HR $n=2$	0.935*	34.0	0.038
$n=3$	0.42*	35.1	0.017
CC TE_{011}	$0.506 \pm .033$	226.5 ± 15	0.136
TE_{012}	$0.406 \pm .027$	230.4 ± 15	0.111

^aBased on $\sigma_{\text{dc}} = 2 \times 10^4$ S/cm.

^bBased on $|\epsilon_t - 1| = 843$.

$$\begin{aligned}
 1/Q_s = \Delta(1/Q) &= 1/Q_{\text{an}} - 1/Q_0 \approx (R_s/\mu_0\omega)F_\sigma(t/\delta) \int_s \mathbf{B}^2 dA_s/U \\
 &= \delta F_\sigma(t/\delta)K', \quad (13b)
 \end{aligned}$$

where R_s is the surface resistance [$R_s=1/\sigma\delta$]. The interface correction factors $F_\varepsilon(t/\delta)$ and $F_\sigma(t/\delta)$ have been given earlier (SC),¹⁵ but approach 1 for $\delta < t/5$, which is the case for the $\text{Cu}_{0.55}\text{Ni}_{0.45}$ calibration sample (except for the larger HR mode $n=1$). In Eq. (13a) magnetic contributions to $\Delta\omega/\omega$ have been neglected because of the negligible magnetic susceptibilities for these samples [$\mu-1 < 10^{-6}$] and the “perfect conductor” correction [Eq. (4)] has not been included for the reasons discussed above. The coefficients I and K' depend on the dimensions of the resonator and on the sample radius and for the HRs are different for each mode n . The values of I and K' determined with the calibration samples are given in Table III. A useful result is the ratio $R \equiv (\Delta\omega/\omega)/\Delta(1/Q)$, which for $F_\varepsilon=F_\sigma=1$ becomes $R = -(\varepsilon_t-1)(I/K')$ providing a direct measure of ε_t independent of δ . For insulating samples ($\delta \gg t$) Eq. (13b) changes to $\sigma t \int_s \mathbf{E}^2 dA_s/\omega U$. The experimental uncertainties for the large HR were estimated from five different calibrations experiments, while three runs were made for the CC. The smaller HR values in Table III are less certain than those for the large HR because of smaller values of Q_0 . For HR mode $n=2$ at 77 K SC¹⁵ found $\Delta\omega/\omega = 0.0166$ for an 0.05 mm Al disk and $\Delta\omega/\omega = 0.0223$ for a 0.33 mm Cu disk. These results are in sharp disagreement with the “perfect conductor” contribution in Eq. (4) that should be proportional to the sample thickness t .

$\Delta(1/Q)$ versus T data is shown for an insulating Si:As sample [$N/N_c=0.72$] in Fig. 3 for HR modes $n=1-3$. Characteristic peaks occur at $T_p \sim 28, 9.5,$ and 6.5 K for $n=1, 2,$ and 3 that are identified with $\delta[f, \sigma(f, T_p)] = t$. This peak represents the crossover between insulating behavior for $T \ll T_p$ and metallic behavior in the skin depth regime ($\delta < t$) for $T > T_p$ and was not observed in an earlier Si:As study⁷ because those measurements were limited to $1.3 < T < 4.2$ K. For $T > T_p$ $\Delta(1/Q) \propto \delta \alpha[\omega\sigma(N, \omega, T)]^{-1/2}$ while for $T < 1/2 T_p$ $\Delta(1/Q) \propto t\sigma(N, \omega, T)$. The values of $\sigma(T_p)$ based on $\delta=t$ are 68, 23, and 14 S/cm for modes $n=1-3$, respectively. The frequency dependence $\sigma(\omega, T=1.5 \text{ K}) \propto \omega^{1.6}$ for $124 < \omega/2\pi < 800$ MHz is shown in the inset. The exponent 1.6 is slightly larger than that in earlier Si:As results, but also represents a different geometry for the E field. This superlinear behavior of $\sigma(\omega, T=1.5 \text{ K})$ is contrasted with the sublinear behavior of Helgren *et al.*³⁸ for insulating amorphous $\text{Nb}_x\text{Si}_{1-x}$ alloys. However, the data in Ref. 38 was for $100 < \omega/2\pi < 1000$ GHz, or two orders of magnitude higher than the data in Fig. 3. Note that $\sigma(\omega, T)$ is decreasing monotonically as T is lowered in the entire range $1.5 < T < 60$ K. A more heavily doped insulating sample [$N/N_c=0.90$] with much larger values of $\sigma_{\text{dc}}(T)$ also shows $\Delta(1/Q)$ increasing as T is lowered for HR modes $n=1-3$, but $\sigma(\omega, T)$ is too large even at 1.5 K and δ remains less than t and no crossover peak is observed. Much lower T would be required to see the crossover.

In Fig. 4 $\Delta\omega/\omega$ and $\Delta(1/Q)$ data are shown for three metallic samples versus T between 1.5 and 4.2 K. The T

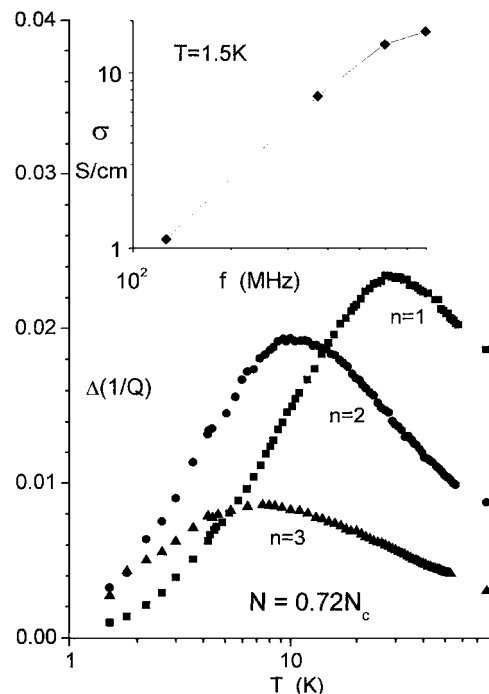


FIG. 3. $\Delta(1/Q)$ vs T for larger HR modes $n=1, 2,$ and 3 for Si:As sample with $N=6.2 \times 10^{18}/\text{cc}$ [$0.72 N_c$]. The peaks occur at $\delta \sim t$ and yield $\sigma=67.8$ S/cm at 28 K for $n=1$, $\sigma=22.9$ S/cm at 10 K for $n=2$, and $\sigma=14.2$ S/cm at 6.7 K for $n=3$. The inset shows $\sigma(T \sim 1.5 \text{ K})$ vs f with an approximate $f^{1.6}$ dependence, a slightly stronger dependence than in Ref. 7.

dependence of both $\Delta\omega/\omega$ and $\Delta(1/Q)$ is very small in this range with the exception of the 13.9 GHz data [TE₀₁₂ mode] which exhibits a 40% increase between 4.2 and 1.5 K and yields an estimate as $T \rightarrow 0$ of $\Delta(1/Q) = 0.0022 \pm 10\%$. There are N -dependent shifts in $\Delta(1/Q)$ for the HR modes with changes in $\sigma_{\text{dc}}(N, T)$. The 9.03 and 10.1 samples show broad maxima in $\Delta(1/Q)$ at $T \sim 10-11$ K and $T \sim 22-24$ K (data not shown) that are consistent with the behavior of $\sigma_{\text{dc}}(N, T)$ for Si:As (Ref. 39) for $T > 4.2$ K. The errors in $\Delta(1/Q)$ increase with HR mode n because of decreased sensitivity of the HR for larger n . The deviations are largest for the $n=4$ HR data. The second significant feature of the data in Fig. 4(a) is the small density dependence of $\Delta\omega/\omega$ compared with that of $\Delta(1/Q)$. $\Delta\omega/\omega$ increases by only 8% as N increases from 9.03 to 17.1, whereas $\Delta(1/Q)$ decreases by a factor of 2.8 for the same change in N . The $\Delta\omega/\omega$ data at 13.9 GHz [TE₀₁₂ mode] exhibit the same features as the data in Fig. 4. If ε_t and δ were both governed by pure Drude behavior in the Hagen-Rubens regime $\omega\tau \ll 1$ then $\Delta\omega/\omega \propto (\sigma_{\text{dc}})^{1/2} \tau / \sqrt{\omega}$ and $\Delta(1/Q) \propto (\sigma_{\text{dc}})^{-1/2}$ and for a fixed ω and τ one expects $\Delta\omega/\omega$ to more than double and $\Delta(1/Q)$ to decrease by more than a factor of 2. The experimental results suggest either ε_t or δ are not obeying pure Drude behavior. Since δ cancels out in the ratio $R = (\Delta\omega/\omega)/\Delta(1/Q)$ one must examine the N -dependence of $R(N, T)$ and from $\delta(N, \omega, T)$ the N -dependence of $\sigma(N, \omega, T)$.

V. DISCUSSION

From Eq. (13b) one obtains δ employing the calibration value K' obtained from the $\text{Cu}_{0.55}\text{Ni}_{0.45}$ calibration sample.

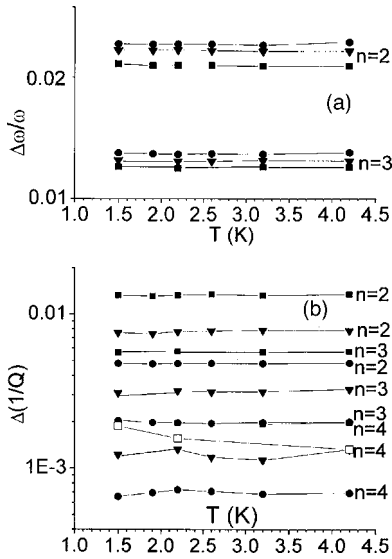


FIG. 4. (a) $\Delta\omega/\omega$ vs T for three metallic samples [9.03 \blacksquare , 10.1 \blacktriangledown , 17.1 \bullet] for larger HR modes 3 and 4. Over a factor of 1.9 increase in N $\Delta\omega/\omega$ only increases by an average factor [modes 2–4] of 1.09. $\Delta(1/Q)$ vs T for these samples for modes $n=2, 3$, and 4. Also shown is TE₀₁₂ data [13.9 GHz, 9.03 \square], the only case with a significant T -dependence for 1.5 K $< T < 4.2$ K. $\Delta(1/Q)$ decreases by a factor [modes 2–4] of 2.8 as N increases by a factor of 1.9. The errors in $\Delta(1/Q)$ increase with n and are $\pm 6\%$ for $n=4$.

Using the classical skin effect result $\delta = (3.16/2\pi)(1/\sigma f_{\text{MHz}})^{-1/2}$ yields $\sigma(N, \omega, T)$. The results for $\sigma(N, \omega, T \sim 1.5$ K) versus reduced density $N/N_c - 1$ for HR frequencies 600 MHz ($n=3$), 800 MHz ($n=4$), and for 13.9 GHz (TE₀₁₂ mode) are given in Fig. 5. Also shown are the Si:As $\sigma_{\text{dc}}(N, T \rightarrow 0)$ values from earlier studies.^{37,39} For the HR modes 3 and 4 $\sigma(N, \omega, 1.5 \text{ K})/\sigma_{\text{dc}}(N, T \rightarrow 0)$ is nearly constant demonstrating the scaling exponent for $\sigma(N, \omega, 1.5 \text{ K})$ is very close to the dc scaling exponent of 1/2. The Cu_{0.55}Ni_{0.45} calibration could introduce an absolute error ($< 20\%$), but this does not affect the scaling exponent of $\sigma(N, \omega, 1.5 \text{ K})$ since the calibration coefficient $K'(\omega)$ is independent of N . The 13.9 GHz data qualitatively shows the same scaling trend, but with greater experimental uncertainties because of the errors in $\Delta(1/Q)$. Sample F ($N/N_c \sim 1.137$) seems too large and sample G ($N/N_c \sim 1.174$) was not measured because it was broken in an earlier experiment. $\Delta(1/Q)$ at 13.9 GHz for sample D ($N/N_c \sim 1.051$) exhibited a T -dependence. A linear- T extrapolation to $T=0$ yielded $\sigma(T=0) \sim 108$ S/cm. Although the 13.9 GHz values are consistently above the dc and 600 MHz values they are only a factor of 1.6 above the former and less than 30% (with exception of sample F) above the 600 MHz values. The frequency dependence of $\sigma(N\omega, T \sim 1.5 \text{ K})$ between 373 MHz and 11.9 GHz is small, but will be discussed further below. The T -dependence of sample D7 at 13.9 GHz is not consistent with that of $\sigma_{\text{dc}}(N, T)$, the latter resulting from $e-e$ interactions as discussed in Refs. 37 and 39.

In Fig. 5(b) the frequency dependence is shown for three samples [D7, 1.051; F4, 1.137; and B18, 1.993] for $T \sim 1.5$ K]. The increase in $\sigma(N, \omega, 1.5 \text{ K})$ with ω is small and

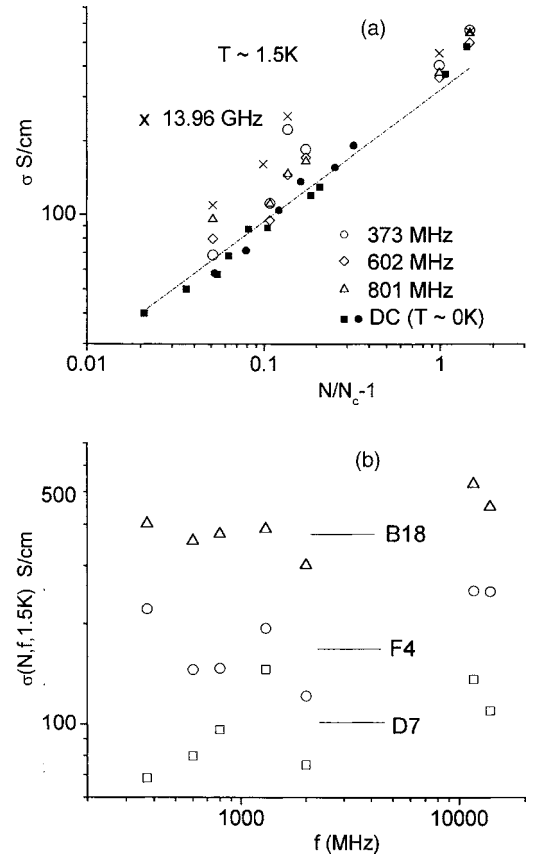


FIG. 5. (a) $\sigma(N, f, T \sim 1.5 \text{ K})$ vs reduced density $N/N_c - 1$ for $f=373$ ($n=2$), $f=602$ ($n=3$), and $f=801$ MHz ($n=4$) and 13.9 GHz. $\sigma_{\text{dc}}(N, T \rightarrow 0)$ values from [Ref. 37 \blacksquare , Ref. 39 \bullet] are also shown. The frequency dependence is small and the microwave conductivity scales with $N/N_c - 1$ with an exponent very close to that for the dc data, namely $s \sim 0.53$. (b) $\sigma(N, f, 1.5 \text{ K})$ vs f for three metallic samples D7, F4, and B18. The lower points at 2010 MHz may result from a calibration error. A 10% increase in K' would increase σ by 21%. At most σ may increase by 25% with f for B18 and perhaps 70% for D7. The deviations from Drude behavior over a factor of 37 in frequency are small.

might be accounted for by (1) interband contributions, (2) $e-e$ interactions, and localized electrons. The increase in the dipole matrix element between the $1S-A_1$ and $1S-T_2$ impurity bands with N is clearly important in determining the interband contribution $\sigma_{\text{ib}}(N, \omega, T)$, however, the infrared results⁸ suggest σ_{ib} will be negligible for $\hbar\omega \ll 1$ MeV. The $e-e$ interaction contribution¹⁴ is $\delta\sigma_{ee} \propto (e^2/\hbar)(kT/\hbar D)^{1/2}(\hbar\omega/kT)^2$ for $\hbar\omega/kT \ll 1$ in the diffusive regime. Note that at 13.9 GHz $\hbar\omega/kT = 0.44$ at 1.5 K. However, the data does not show the $D(N)^{-1/2} N$ -dependence of $\delta\sigma_{ee}$. Furthermore, for the $N=1.051N_c$ sample [D7] the T -dependence has the wrong sign, namely Fig. 5 shows $\sigma(N, \omega, T)$ getting smaller as $T \rightarrow 0$ which is contrary to the $\delta\sigma_{ee}$ prediction. This T -dependence is qualitatively consistent with a contribution from localized electrons (as in Fig. 3), however, it is not clear whether the ω -dependence is consistent. The two-component model⁴⁰ for the uncompensated case yields $N_{\text{loc}} + N_i = N$ and the itinerant electron density $N_i = \lambda N_c (N/N_c - 1)^{1/2}$ with $\lambda \sim 2$ for the weakly compensated

case. For $N=1.051N_c$ 60% of the electrons are localized and a conductivity of the form

$$\sigma_{\text{total}}(N, \omega, T) = \sigma_i + N_{\text{loc}}f(\omega, T) \quad (14)$$

might be expected, where the first term is the metallic term showing BD behavior and the second term is that from the localized electrons where $f(\omega, T)$ shows a stronger ω -dependence than σ_i . However for larger N N_{loc} becomes much smaller. For the $N=1.993N_c$ sample (B18) $N_{\text{loc}} < 0.02N_c$ and the second term in Eq. (14) would be negligible. It is only in the lower part of the scaling regime $N_c < N < 2N_c$ where there are localized electrons that might give rise to a stronger ω -dependence. The data in Fig. 5 suggest for $N \geq 2N_c$ the ω -dependence above σ_{dc} is smaller than just above N_c . This scaling regime consisting of both N_i and N_{loc} represents that of an inhomogeneous conductor where $\sigma(N, \omega, T \rightarrow 0)$ will be a function of \mathbf{r} . However, at the critical point as $T \rightarrow 0$, $N_i \rightarrow 0$ and for $\hbar\omega \gg kT$, $\sigma_{\text{total}} \propto N_{\text{loc}}(\omega)^{1/2}$ as demonstrated for amorphous $\text{Nb}_x\text{Si}_{1-x}$.⁹

Should these small increases in $\sigma(N, \omega, 1.5 \text{ K})$ with ω in Fig. 5 be considered seriously? They depend critically on the calibration with the $\text{Cu}_{0.55}\text{Ni}_{0.45}$ sample. If the surface conductivity σ_{sur} within δ of the surface is smaller than σ_{bulk} because of increased surface scattering the $K'(\omega) \propto (\sigma_{\text{sur}}/\sigma_{\text{bulk}})^{1/2}$. For the 13.9 GHz data a factor $\sigma_{\text{sur}}/\sigma_{\text{bulk}} = 1/2$ would increase K' by $\sqrt{2}$ and reduce the 13.9 GHz σ values by a factor of 2 making them *smaller* than the $\sigma_{\text{dc}}(N, T \rightarrow 0)$ values in Fig. 5. *This seems very unlikely, but cannot be ruled out experimentally with our approach.* What can be concluded is any ω -dependence [$124 \text{ MHz} < f < 13.9 \text{ GHz}$] is small and that deviations from Drude behavior are small.

The ratio $R = (\Delta\omega/\omega)/\Delta(1/Q)$ [proportional to $-(\epsilon_r - 1)$] versus $N/N_c - 1$ is shown in Fig. 6. In Fig. 6(a) the results for the larger HR are shown for modes $n=2$ (373 MHz), $n=3$ (602 MHz), and $n=4$ (801 MHz). The open symbol values are the uncorrected values while the closed symbols are $R_c = R[F_\sigma(t/\delta)/F_\epsilon(t/\delta)]$. Note that the t/δ correction is positive for small values of $N/N_c - 1$ and negative for large values of $N/N_c - 1$. From SC¹⁵ the correction is positive for $t/\delta < 2.03$, negative for $2.03 < t/\delta < 4.9$, and less than 2% for $t/\delta > 4.5$. Normally one expects R to increase somewhat with frequency and this is borne out for a majority of the samples. The trend is clear and is supported by the R values in Fig. 6(b) for the CC and the smaller HR. This trend is given by the dot-dash lines in Figs. 6(a) and 6(b) with a slope of 0.3. For pure BD behavior one should get $R_c \propto (\omega_p\tau)^2 \propto (N/N_c - 1)^{1/2}$. The slower dependence implies a correction to BD behavior, most likely from an interband contribution $\epsilon_{i,\text{ib}}$.

The Si:P infrared data of Gaymann *et al.*⁸ permits a direct determination of $\epsilon_{i,\text{ib}}$. The data in their Fig. 5 has been analyzed to obtain the interband conductivity $\sigma_{\text{ib}} = \sigma(E, 10 \text{ K}) - \sigma_{\text{Drude}}(E, \tau)$ where $\sigma_{\text{Drude}}(E, \tau) = \sigma_0(N)/[1 + (E/E_c)^2]$ and $E_c = 19.6 \text{ meV}$ as estimated from the data for the 7.3×10^{18} sample. This E_c corresponds to $\tau = 3.36 \times 10^{-14} \text{ s}$, a value only 4% larger than that obtained from $\sigma_{\text{dc}}(T=0) = 260 \text{ S/cm}$ for $N=2N_c$. σ_0 is approximated from the E

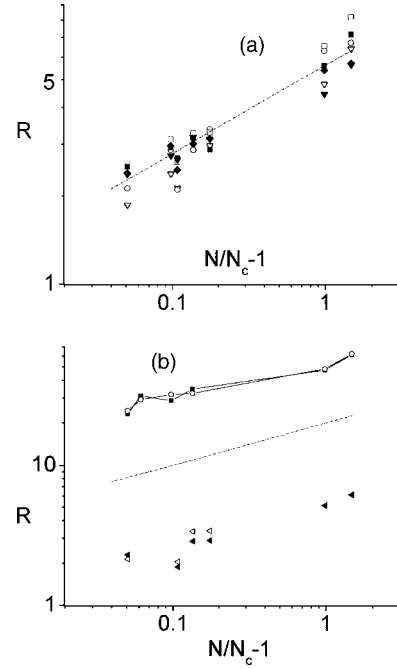


FIG. 6. (a) The ratio $R = [(\Delta\omega/\omega)/\Delta(1/Q)]$ and $R_c = R[F_\sigma(t/\delta)/F_\epsilon(t/\delta)]$ vs $N/N_c - 1$ for the large HR modes $n=2, 3$, and 4. The open symbols are R and the closed symbols R_c . F_σ/F_ϵ is greater than one for small $N/N_c - 1$ and less than one for $N/N_c - 1 \sim 1$. The dot-dash line has a slope of 0.3. (b) The ratio R for the TE_{011} [■] and TE_{012} [◇] modes where $t/\delta > 6$ and the interference corrections are small. Values of R and R_c for the smaller HR mode $n=3$ that are comparable to the values for the larger HR in (a). Note the R values for the CC are close to a factor of 10 larger than those for the HRs. The dot-dash line has a slope of 0.3.

$= 1 \text{ meV}$ value. $\sigma_{\text{ib}}(E, T=10 \text{ K})$ is shown in Fig. 7(a). There are two important features for $\sigma_{\text{ib}}(E)$: (1) the $1s - A_1 \rightarrow 1s - T_2$ band transition, with a peak in the 6–8 meV region increases strongly with N from 4.5 to 7.3; and (2) the $1s - A_1 \rightarrow \text{Si}$ conduction band transition (starting for $E > 20 \text{ meV}$ and peaking near 45 meV) decreases significantly from 4.5 to 7.3 being down by a factor of 2.5 from 4.5 to 7.3. From the Kramers-Kronig result

$$\epsilon_{\text{ib}}(E') = 8P \int_0^\infty \sigma_{\text{ib}}(E) dE/[E^2 - E'^2]. \quad (15)$$

Setting $E' \sim 0$ this integral is evaluated numerically for an upper limit of 30 meV and yields 31.5, 44.1, and 45.9 for the 4.5, 5.2, and 7.3 cases, respectively. Most of the contribution comes from $E < 12 \text{ meV}$. Even though the peak of σ_{ib} is 60% higher for 7.3 than for 5.2 the peak is at 8 meV for 7.3 compared to 6 meV for 5.2 and the low energies dominate in Eq. (15). In Fig. 7(b) values of ϵ_i versus $N/N_c - 1$ from the CC TE_{011} (□) and TE_{012} (×) are slightly larger than those obtained with the larger HR by close to a factor < 1.8 and seem too large by this factor compared to the values in Table I. The dot-dash line, with a slope of 1/2, the pure Drude prediction, is clearly more rapid than the data and one would have to add $\epsilon_{i,\text{ib}}$ to the Drude result $-(\omega_p\tau)^2$. The CC higher frequency data might be viewed as supporting a slope near

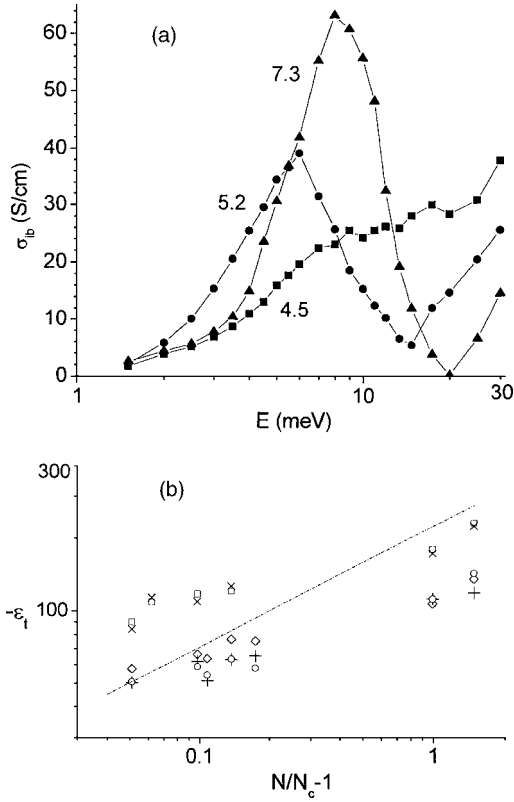


FIG. 7. (a) The interband $\sigma_{ib} = \sigma(N, E, T \sim 10 \text{ K}) - \sigma_{\text{Drude}}(E)$ [$E_r = \hbar/\tau = 19.6 \text{ meV}$] obtained from Gaymann *et al.* (Ref. 8) for $4.5, 5.2,$ and $7.3 \times 10^{18}/\text{cc}$ Si:P metallic samples. A Kramers-Kronig analysis yields $\epsilon_{ib}(E \ll 1 \text{ meV})$ of 31, 44, and 46 for the 4.5, 5.2, and 7.3 samples, respectively, showing that ϵ_{ib} is a significant fraction of $\epsilon_{\text{Drude}} = -(\omega_p \tau)^2$. (b) Values of ϵ_t for Si:As using $-\epsilon_t = 843(R/R_{\text{CuNi}})$, thus setting $\epsilon_{ib} = 0$ for the $\text{Cu}_{0.55}\text{Ni}_{0.45}$ calibration sample and using R_{CuNi} values from Table III. The smaller values come from the R values from Fig. 6(a) for modes 2 [\diamond], 3 [$+$], and 4 [\square]. The larger values come from CC modes TE_{011} [\square] and TE_{012} [\times]. The 60% larger values for the CC case are not easily explained. The dot-dash line shows the expected slope for pure Drude behavior. The actual observed slopes are closer to 0.3, indicating an interband contribution for Si:As, as suggested by the results in (a).

$1/2$ for $N/N_c - 1 < 0.14$ followed by a droop at the two largest values of N/N_c . However, the HR results are less clear and could support a smaller slope near 0.3 over the entire range of $N/N_c - 1$. However, the HR data scatter is large enough to make any scaling exponent claims problematic. All that can be said is the ϵ_t result is consistent with a Drude plus interband contribution to yield a resulting $\epsilon_t(N)$ smaller than $-(\omega_p \tau)^2$ because of $\epsilon_{t,ib}$ and $\epsilon_h = 11.4$. However, the $\epsilon_{t,ib}$ contribution for Si:As is not known, but should be within a factor of 2 of the Si:P values.

The difference (factor < 1.8) between the CC and HR results is outside the experimental error limits and may represent a problem with the calibration procedure. Possible reasons are (1) $\text{Cu}_{0.55}\text{Ni}_{0.45}$ is not a good Drude metal and shows a frequency-dependent $\epsilon_t(\omega)$ that changes between 1 and 11.4 GHz; (2) as discussed in Sec. II C the difference between E_θ (CC) and E_r (HR) is important and the extra term in the stored energy W for $\Delta(1/Q)$ resulting from the induced

magnetic dipole field which is present for $\Delta(1/Q)$, but not for $\Delta\omega/\omega$; (3) The CC results are correct, implying ϵ_t for $\text{Cu}_{0.55}\text{Ni}_{0.45}$ is closer to 1680 rather than 840 implying the HR values are too small by a factor of 2. This problem is not easily resolved. Reason (1) seems unlikely but could only be ruled out with additional measurements of a known sample with reasonably large ϵ_t and no dispersion. Reason (2) is possible and the large frequency shifts may suggest essential corrections to the perturbation fields used in calculating $\Delta(1/Q)$. However, the good agreement of $\sigma(N, \omega, T = 1.5 \text{ K})$ with Drude behavior and only slight increases above σ_{dc} as shown Fig. 5 would appear to argue against this. However, because of the difference between K'_{expt} and K'_{calc} for the CC this cannot be ruled out. The magnetic dipolar contribution to the stored W would make this discrepancy worse. Reason (3) is at odds with the expected magnitude of $-(\omega_p \tau)^2$ (see Table I) and with values of $4\pi\sigma_{\text{dc}}\tau$.

Although $\epsilon_1(N, \omega, T = 1.5 \text{ K})$ is negative for the metallic samples studied in this work in the Hagen-Rubens regime ($\omega\tau \ll 1$) it is known that $\epsilon_1(\omega)$ can cross zero several times at much higher frequencies. Lee and Heeger⁴¹ studied the reflectivity $R(\omega)$ of the metal-insulator system metallic polypyrrole doped with PF_6 over a broad frequency range 8 to $5 \times 10^4 \text{ cm}^{-1}$. They report zero crossing of $\epsilon_1(\omega)$ at 20 and $1.3 \times 10^4 \text{ cm}^{-1}$ and explain their results with a localization-modified Drude model. The higher crossing is at the screened plasma frequency $(\omega_p^2/\epsilon_\infty)^{1/2}$. However, even in the $\omega\tau \ll 1$ regime Eq. (2) predicts a zero crossing of $\epsilon_1(N, \omega)$ at a density $N > N_c$ given by

$$\epsilon_h + \delta\epsilon_{ib}(N, \omega\tau \ll 1) = [\omega_p \tau(N = 2N_c)]^2 (N/N_c - 1)^{1/2}. \quad (16)$$

$\delta\epsilon_{ib}(N, \omega\tau \ll 1)$ is not accurately known for N barely above N_c but could be smaller than ϵ_h . Neglecting it and using $\epsilon_h = 11.4$ and $[\omega_p \tau(N = 2N_c)]^2 = 78.6$ (see Table I) yields $N_{\text{co,min}} = 1.02N_c$. N_{co} will increase with $\delta\epsilon_{ib}$. This suggests a more complex behavior of $\epsilon_1(N, \omega\tau \ll 1)$ for N just above N_c where a majority of the carriers are localized. At $N = 1.02N_c$ $N_{\text{loc}} = 6.29 \times 10^{18}/\text{cm}^3$ and $N_i = 2.49 \times 10^{18}/\text{cm}^3$. Equation (2) does not take account of contributions to ϵ_1 from the localized electrons. However, these corrections would be analogous to those in the localized-modified Drude model in Ref. 41.

VI. CONCLUSIONS

The HR results demonstrate, despite the more complex field distribution within the HR because of the finite, shorted helix, that this experimental approach can yield reliable values of the microwave conductivity and transverse dielectric response when the HR is properly calibrated. The first few HR modes $n = 1 - 4$ can yield data over a frequency range of more than six. The HR avoids the mode degeneracy problem associated with the CC TE_{01n} and TM_{11n} modes and permits measurements down to the low 100-MHz realm. The results also demonstrate that the “perfect conductor” contribution to $\Delta\omega/\omega$ is not relevant to the present results in the skin depth regime, contrary to other work.

Far into the Hagen-Rubens regime the results show the microwave conductivity $\sigma(N, \omega, 1.5 \text{ K})$ very close to $\sigma_{dc}(N, T \rightarrow 0)$ and deviations from Drude behavior are small over a factor of 37 in ω . Just above N_c $\delta\sigma(N, \omega, 1.5 \text{ K})$ may increase by 70%, possibly from inhomogeneity and photon-assisted hopping observed from insulating samples. The ratio $R = [(\Delta\omega/\omega)/\Delta(1/Q)]$ provides a good measure of the dielectric response $\epsilon_i(N, \omega, 1.5 \text{ K})$. ϵ_i shows a large Drude contribution from plasmons, but also shows a correction from an interband contribution from $1s-A_1 \rightarrow 1s-T_2$ transitions (and $1s-A_1 \rightarrow$ conduction band transitions) as inferred from the infrared data. The Drude contribution to $\epsilon_i \propto -(\omega_p\tau)^2 = -4\pi\sigma_{dc}\tau$ is qualitatively consistent with the

$\sigma_{dc}(N, T \rightarrow 0)$ scaling results and a τ independent of N . This is consistent with the scaling of the Drude portion coming from $\omega_p^2 \propto N_i \sim 2N_c(N/N_c - 1)^{1/2}$. The present results can be adequately explained without contributions from weak-localization or $e-e$ interactions.

ACKNOWLEDGMENTS

This work was supported by NSF Grant DMR-9803969. The authors thank M. Bocko for the use of HP network analyzers and J. Waldman for the use of his facilities. T.G.C. acknowledges useful discussions with S. Sridhar.

*Present address: Korea Electrotechnology Research Institute, Seong-Joo-Dong 28-1 Changwon, Kyung-Nam, Korea 641-120.

¹R. F. Milligan, T. F. Rosenbaum, R. N. Bhatt, and G. A. Thomas, in *Electron-Electron Interactions in Disordered Systems*, edited by A. L. Efros and M. Pollak (North-Holland, Amsterdam, 1985), p. 231.

²M. P. Sarachik, in *Metal-Insulator Transitions Revisited*, edited by P. P. Edwards and C. N. R. Rao (Taylor and Francis, London, 1995), p. 79.

³T. G. Castner, in *Phase Transitions and Self-Organization in Electronic and Molecular Networks*, edited by J. C. Phillips and M. F. Thorpe (Kluwer Academic/Plenum Publishers, New York, 2001), p. 263.

⁴T. G. Castner, Phys. Rev. B **61**, 16596 (2000).

⁵H. F. Hess, K. DeConde, T. F. Rosenbaum, and G. A. Thomas, Phys. Rev. B **25**, 5578 (1982).

⁶J. S. Brooks, O. G. Symko, and T. G. Castner, Jpn. J. Appl. Phys., Part 1 **26**, Suppl. 26-3, 721 (1987).

⁷R. J. Deri and T. G. Castner, Phys. Rev. Lett. **57**, 134 (1986); M. Migliuolo and T. G. Castner, Phys. Rev. B **38**, 11593 (1988).

⁸A. Gaymann, H. P. Geserich, and H. V. Löhneysen, Phys. Rev. Lett. **71**, 3681 (1993); Phys. Rev. B **52**, 16486 (1995).

⁹H. L. Lee, J. R. Carini, D. V. Baxter, and G. Grüner, Phys. Rev. Lett. **80**, 4261 (1998).

¹⁰F. A. D'Altroy and H. Y. Fan, Phys. Rev. **103**, 1671 (1956).

¹¹D. W. Mahaffey and D. A. Jerde, Rev. Mod. Phys. **40**, 710 (1968).

¹²M. Dressel and G. Gruner, *Electrodynamics of Solids, Optical Properties of Electrons in Matter* (Cambridge University Press, Cambridge, 2002).

¹³S. Sridhar and W. L. Kennedy, Rev. Sci. Instrum. **59**, 531 (1988).

¹⁴B. Altshuler and A. Aronov, in *Electron-Electron Interactions in Disordered Systems*, edited by A. Efros and M. Pollak (North-Holland, Amsterdam, 1985).

¹⁵K. J. Song and T. G. Castner, Rev. Sci. Instrum. **72**, 1760 (2001).

¹⁶R. Diehl, D. M. Wheatley, and T. G. Castner, Rev. Sci. Instrum. **67**, 3904 (1996).

¹⁷J. Müller, Z. Hochfr. Techn. Elekt. **54**, 157 (1939).

¹⁸J. Schwinger, MIT Rad. Lab. Report 43-44 (unpublished).

¹⁹H. A. Bethe and J. Schwinger, N.D.R.C. Report No. D1-117, Cornell Univ., 1943 (unpublished).

²⁰W. Hauser, *Introduction to the Principles of Electromagnetism* (Addison-Wesley, Reading, 1971), p. 512.

²¹J. G. Linhart, I. M. Templeton, and R. Dunsmuir, Br. J. Appl. Phys. **7**, 36 (1956).

²²T. Kohane and M. H. Sirvetz, Rev. Sci. Instrum. **30**, 1059 (1959).

²³J. O. Artman and P. E. Tannenwald, J. Appl. Phys. **26**, 1124 (1955).

²⁴E. G. Spencer, R. C. LeCraw, and F. Reggia, Proc. Inst. Radio Eng. **44**, 790 (1956).

²⁵W. Von Aulock and J. H. Rowen, Bell Syst. Tech. J. **36**, 427 (1957).

²⁶H. Seidel and H. Boyet, Bell Syst. Tech. J. **37**, 637 (1958).

²⁷E. G. Spencer, R. C. LeCraw, and L. A. Ault, J. Appl. Phys. **28**, 130 (1957).

²⁸R. A. Waldron, Proc. Inst. Electr. Eng. **107C**, 272 (1960).

²⁹J. Slater, Rev. Mod. Phys. **18**, 441 (1946).

³⁰M. E. Brodwin and M. K. Parsons, J. Appl. Phys. **36**, 494 (1965).

³¹O. Klein, S. Donovan, M. Dressel, and G. Gruner, Int. J. Infrared Millim. Waves **14**, 2423 (1993).

³²D. N. Peligrad, B. Nebendahl, C. Kessler, and M. Mehring, Phys. Rev. B **58**, 11652 (1998).

³³Z. Zhai, C. Kusko, N. Hakim, S. Sridhar, A. Revcolevschi, and A. Vietkine, Rev. Sci. Instrum. **71**, 3151 (2001).

³⁴J. R. Pierce, *Traveling Wave Tubes* (Van Nostrand, Princeton, 1950).

³⁵N. P. Ong, J. Appl. Phys. **48**, 2935 (1977).

³⁶K. S. Champlin and R. R. Krongard, IRE Trans. Microwave Theory Tech. **MIT-9**, 545 (1961).

³⁷W. N. Shafarman, D. W. Koon, and T. G. Castner, Phys. Rev. B **40**, 1216 (1989).

³⁸E. Helgren, G. Grüner, M. R. Ciofalo, D. V. Baxter, and J. P. Carini, Phys. Rev. Lett. **87**, 116602 (2001).

³⁹P. F. Newman and D. F. Holcomb, Phys. Rev. B **28**, 638 (1983).

⁴⁰T. G. Castner, Phys. Rev. B **67**, 193202 (2003).

⁴¹K. Lee and A. J. Heeger, Phys. Rev. B **68**, 035201 (2003).